

# A Study on Characteristics of Ground Motion during The 2011 Off the Pacific Coast of Tohoku Earthquake



**H. Dohi & K. Yoshida**

*NTT Facilities, Japan*

**S. Matsuda**

*Kansai University, Japan*

**M. Kawano**

*former Kyoto University, Japan*

## **SUMMARY:**

In this paper, to examine the validity of the ground motion model presented on the basis of wave propagation theory and source kinematics, some ground motions have been made in the case of the 2011 off the Pacific coast of Tohoku Earthquake, M9. Their time histories of wave form and response spectra have been compared with the ones of the observed earthquake ground motions at two sites. Then the key parameters influencing characteristics of ground motion and structural response have been extracted by this simulation test. They are site geological structure, focal distance, geometric relation between site and source, asperity size and distribution on the fault plane.

*Keywords: Prediction of ground motion, Simulation test, Ground motion model, Wave propagation theory*

## **1. INTRODUCTION**

In a previous paper, the prediction model of ground motion has been presented on the basis of wave propagation theory and source kinematics. In this modelling of ground motion, the rupture process for a unit event on the fault plane has been idealized as an impulse response of elastic membrane. This dynamic response has been applied for modelling source rupture process as a unit slips function with  $\omega^2$  spectral characteristics. The soil ground model for source-site path has been presented as a multi-layered half-space which consists of some soil layers overlying a semi-infinite random medium. The prediction model of ground motion has been presented by Green's function of soil ground model and the source rupture process model. The excellent prediction potential of this ground motion model has been verified through a simultaneous simulation test against the observed ground motions at some sites during the 1995 Hyogo-ken Nanbu Earthquake of magnitude 7.2.

In this paper, to examine the validity of this ground motion model, some ground motions have been made in the case of the 2011 off the Pacific coast of Tohoku Earthquake, M9. Their time histories of wave form and response spectra have been compared with the ones of the observed earthquake ground motions at two sites. Then the key parameters influencing characteristics of ground motion and structural response have been extracted through this simulation test.

## **2. EARTHQUAKE DATA AND SEISMIC RECORDING SITES**

The seismograms of ground motion at Sendai and Shinjuku sites during the 2011 off the Pacific coast of Tohoku Earthquake have been used for the simultaneous simulation test. Fig. 2. shows the causative fault and the location of the two observation sites, Sendai (N38.267°, E140.878°) and Shinjuku (N35.682°, E139.688°). The fault location is N39.885° E144.374°. Kamae and Kawabe described the fault model as shown in Fig. 2. There are 5 asperity areas on the fault plane. In this paper, they have been used for fault parameters, fundamentally. Besides, the modified fault model has been presented for the prediction of ground motions, which has back ground area except the 5 asperities areas. The

fault parameters are listed in Table 2. The magnitude of the earthquake was estimated to be  $M=9$ . The total seismic moment was  $M=1.235 \times 10^{22}$  N m.

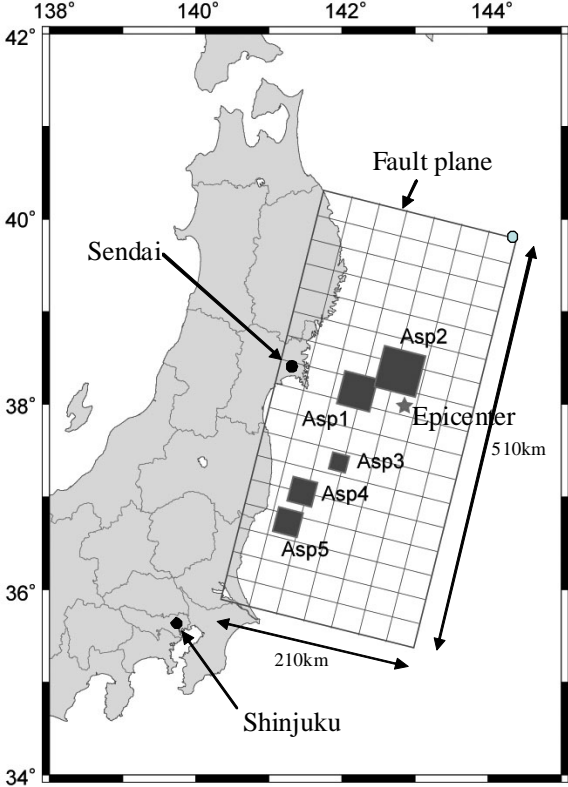


**Figure 2.** Location of observation sites and fault plane (Kamae & Kawabe)

**Table 2.** Fault parameters

	Asp1	Asp2	Asp3	Asp4	Asp5	Back ground
Strike	N195° E					
Dip angle	13°					
Area	40x40km <sup>2</sup>	50x50km <sup>2</sup>	20x20km <sup>2</sup>	30x30km <sup>2</sup>	30x30km <sup>2</sup>	1,01,200km <sup>2</sup>
Seismic moment	4.93x10 <sup>20</sup> Nm	1.10x10 <sup>21</sup> Nm	8.80x10 <sup>19</sup> Nm	1.19x10 <sup>20</sup> Nm	2.58x10 <sup>20</sup> Nm	1.029x10 <sup>22</sup> Nm
Rake angle	90°					
Rupture velocity	2.7km/s					

**3. GEOLOGICAL SEDIMENT STRUCTURE AND PROPERTY OF OBSERVATION SITE**

The geological structures of shallow surface soil sediment layers (GL – GL-50m) at Sendai and Shinjuku sites were investigated in detail on the basis of PS logging and boring data. The profiles of shear wave velocities in the deeper geological structure including the basement bedrock refer to the investigation by Kobayashi et al., Seo et al., and Koketsu et al. The lithosphere region from source to basement bedrock has been modelled as a random medium [Kawano et al.]. The geological structures from source to site of Sendai and Shinjuku sites are summarized in Table 3.1. and 3.2. Those data are used to calculate the three-dimensional Green's functions from the sub-faults to sites. Fig. 3.1. and Fig. 3.2. show the one-dimensional amplification factors of surface soil sediment layers (dotted lines) and the entire soil sediment layers from bedrock to surface (solid line) at the sites, respectively.

The large components are recognized in the short period range less than 0.4 sec in common with the two sites. They reflect the amplification factors of their shallow surface soil sediment layers. Some large components are also clearly recognized in the long period about 2 sec at Sendai site, and about 7 sec, 3 sec and 2 sec at Shinjuku site, respectively. They correspond with the predominant periods of deeper soil sediment layers.

**Table 3.1.** Geological data of Sendai site

Depth(m)	Vp(m/sec)	Vs(m/sec)	Density (g/cm <sup>3</sup> )	Damping factor (%)
0.0~1.40	320	210	1.60	1.00
1.40~2.00	320	210	2.00	1.00
2.00~6.70	870	360	2.00	1.00
6.70~14.85	1860	500	1.80	1.00
14.85~16.60	1860	500	1.85	1.00
16.60~20.00	1860	500	1.78	1.00
20.00~26.00	1860	670	1.78	1.00
26.00~28.80	1860	760	1.78	1.00
28.80~30.10	1860	760	1.80	1.00
30.10~34.80	1860	760	1.78	1.00
34.80~39.40	1860	640	1.80	1.00
39.40~44.60	1860	640	1.78	1.00
44.60~48.15	1860	640	1.80	1.00
48.15~95.00	1860	640	1.78	1.00
95.00~140.0	2040	790	1.90	1.00
140.0~230.0	2220	940	2.00	0.50
230.0~560.0	2510	1520	2.10	0.50
560.0~900.0	3880	1640	2.20	0.50
900.0~	5670	3210	2.30	0.25

**Table 3.2.** Geological data of Shinjuku site

Depth(m)	Vp(m/sec)	Vs(m/sec)	Density (g/cm <sup>3</sup> )	Damping factor (%)
0.0~7.0	900	180	1.60	1.00
7.00~11.00	900	260	1.60	1.00
11.00~26.0	1500	260	1.90	1.00
26.0~110.0	1700	420	2.00	1.00
110~410	1960	720	2.00	1.00
410~1330	2300	950	2.02	0.50
1330~2530	2910	1370	2.15	0.50
2530~16500	5450	3110	2.71	0.50
16500~	6280	3680	2.89	0.25

----- : Border line of surface soil layers and deeper soil layers  
 Vp : P-wave velocity  
 Vs : S-wave velocity

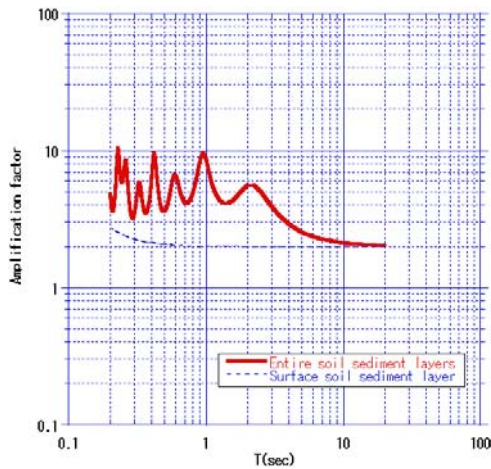


**Figure 3.1.** Site amplification factor of Sendai site

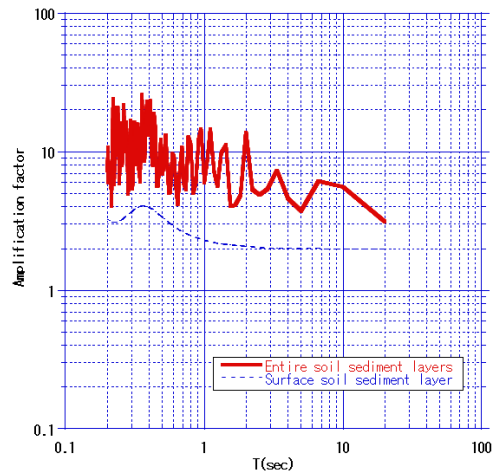


**Figure 3.2.** Site amplification factor of Shinjuku site

#### 4. PREDICTION MODEL OF GROUND MOTION

The entire soil sediment layers including the lithosphere from source to bedrock have been modelled by a three-dimensional multi-layered half-space overlying a random medium as shown in Fig. 4. The Green's functions from all the sub-faults on each fault plane to the interest sites have been calculated using wave propagation theory. The ground motion at each site is expressed by the convolution of the Green's functions and the source model.

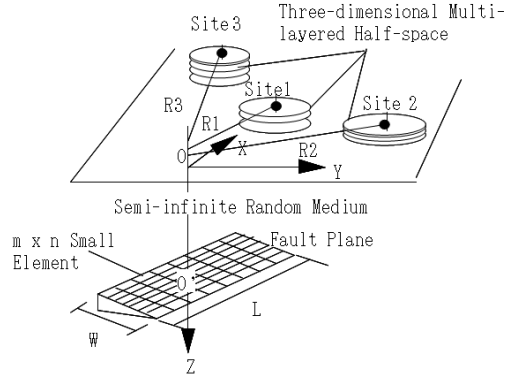


**Figure 4.** Geometric relation between causative fault and sites

#### 4.1. Source Model

The rupture process for a unit event on the sub-fault is idealized by an impulse response of the dynamic behaviour of a continuous membrane (Kawano et al.). This dynamic response is used in source modelling as a slip function with the  $\omega^{-2}$  spectral characteristics. The high frequency waves are assumed to be emitted from the spatially and temporally random small-scale fault heterogeneity as the rupture propagates over the fault plane. The seismic moment distribution to describe source model has been estimated by the slip vectors on the fault elements, which are obtained by dividing the entire fault plane in to 119 (17 x 7) small elements as shown in Fig. 2. The elementary source including the starting and stopping effects of the rupture front has been described by the slip function and slip vectors with spatial and temporal random fluctuation due to heterogeneous asperity on the fault element (Kawano et al.). Then the source rupture growth process of a large event may be modelled by a sum of the elementary sources occurring with the random lagged times  $t_r(\xi_{(m)})$  to rupture-events on the entire fault plane as

$$M_{0(m)}(t) = \frac{\overline{M}_{0(m)}}{T_{(m)}} \int_0^{T_{(m)}} f_m(\zeta) g_m(t - \zeta) d\zeta \quad (4.1)$$

$$\overline{M}_{0(m)} = \mu \Delta u'_{(m)} L_{(e)} W_{(e)} \quad (4.2)$$

$$f_m(\zeta) = \sum_{j=1}^{N_1} f_j \frac{T_{(m)}}{\Delta T_j} B(\zeta - T_j; \Delta T_j) \quad (4.3)$$

$$B(\zeta; \Delta T_j) = \begin{cases} 1 & ; 0 \leq \zeta \leq \Delta T_j \\ 0 & ; \zeta < 0 \text{ or } \Delta T_j < \zeta \end{cases}$$

$$T_1 = 0, T_{j+1} = T_j + \Delta T_j, \sum_{j=1}^{N_1} \Delta T_j = T_{(m)}, \sum_{j=1}^{N_1} f_j = 1$$

$$g_m(t) = \sum_{k=1}^{N_2} g_k \left\{ \frac{1}{2} \left( 1 + \tanh \left[ \frac{4(t - \tau_k)}{\Delta \tau_k} \right] \right) \right\} \quad (4.4)$$

$$\tau_1 = 0, \tau_{k+1} = \tau_k + \Delta \tau_k, \sum_{k=1}^{N_2} \Delta \tau_k = \tau_{(m)}, \sum_{k=1}^{N_2} g_k = 1$$

where  $f_m$  and  $g_m$  are the spatial slip function with boxcar function and the temporal slip function with smoothed ramp function,  $M_{0(m)}$ ,  $\Delta u'_{(m)}$  and  $\mu$  are seismic moment, average slip displacement and shear rigidity at the  $m$ th fault element,  $\Delta T_j$  and  $\Delta \tau_k$  are the fluctuating rupture time and rise time due to the small-scale heterogeneous asperity on the fault plane,  $\omega$  is the angular frequency.  $N_1$  and  $N_2$  are set to be 5 (Kawano et al.).

## 4.2. Synthetic Ground Motion at Sites

The ground motions at the two sites are presented as a sum of all the seismic wave motions radiated when the rupture front reaches the centers of the fault elements as

$$u_n(\mathbf{x}, \omega) = \sum_{m=1}^N M_{(m)pq}(\omega) \frac{\partial}{\partial \xi_q} G_{np}(\mathbf{x}; \omega; \xi_{(m)}, 0) \quad (4.5)$$

$$M_{(m)pq}(\omega) = R_{pq(m)} M_{0(m)}(\omega)$$

where  $R_{pq}$  is radiation pattern.  $G_{np}(\mathbf{x}, \omega; \xi_{(m)}, 0)$  is the Fourier transform of  $G_{np}(\mathbf{x}, t-\tau; \xi_{(m)}, 0)$  which is the  $n$ th component of displacement at position  $\mathbf{x}$  and time  $t-\tau$  caused by an instantaneous force of a unit amplitude applied in the  $p$  direction at the reference point  $\mathbf{x}_{(m)}$  and time  $t=0$  (Aki, K. et al.).  $M_{(m)pq}(\omega)$  is the elementary seismic moment tensor of the  $pq$  component.  $M_{(m)}(\omega)$  is the Fourier transform of  $M_{(m)}(t)$ .

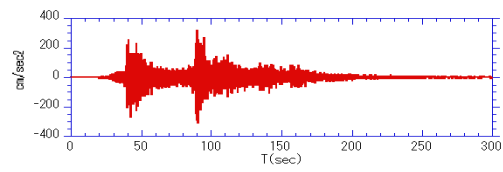
## 5. VERIFICATION OF PREDICTED SITE RESPONSE

The verification for the synthetic ground motion in Section 4 has been performed for the seismograms recorded at the Sendai and Shinjuku sites during the 2011 of the Pacific coast of Tohoku Earthquake. The Sendai site is located in nearer place from the fault plane and the distance from hypocenter to the site is about 150 km. On the other hand, the Shinjuku site is located in about 350 km from hypocenter.

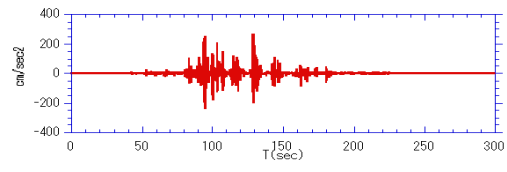
Fig. 5.1. and Fig. 5.2. show the comparisons of the observed and synthetic acceleration time histories of three component ground motions at Sendai and Shinjuku sites. They are fundamentally similar to the observed ones in the main dynamic part of the time histories at both sites. However, there are some differences between observed and synthetic ones in the succeeding wave group. It may be considered that reason is the effects of complex fault rupture process and structure of uneven ground.

Fig. 5.3. shows the comparisons of the observed and synthetic velocity response spectra with 5% damping ratio of three component ground motions at Sendai and Shinjuku sites. The synthetic ground motion amplitude is similar to observed one in wide period range 0.1 - 10s. The response spectra at two sites are excited in the period range 1.0 - 3.0s, because the site amplification factors have large component in this period range as shown in Fig. 3.1. and Fig. 3.2.

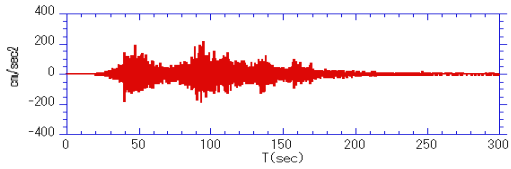
The above results have indicated that if the site geological structure from surface to deeper layer, geometric relation between site and source, and asperity on a fault plane were definite, the characteristics of ground motion could be mainly described.



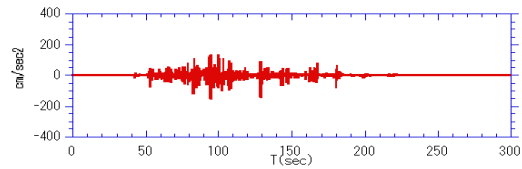
OBS.(N344E)



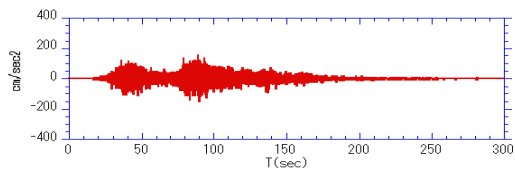
SYN.(N344E)



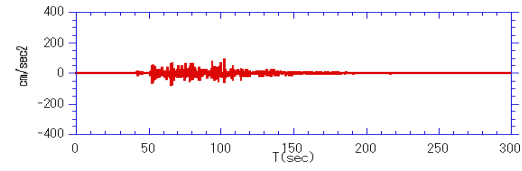
OBS.(N74E)



SYN.(N74E)

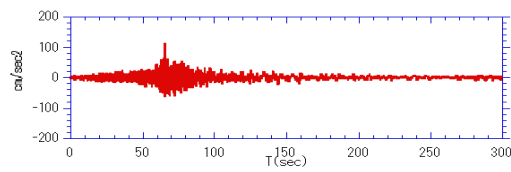


OBS.(UD)

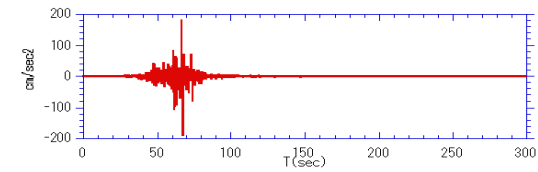


SYN.(UD)

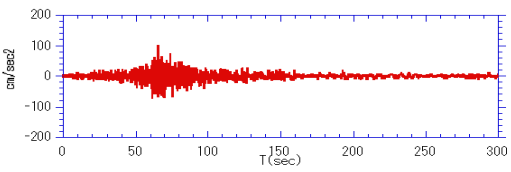
**Figure 5.1.** Comparison of observed and synthetic acceleration time histories for Sendai site



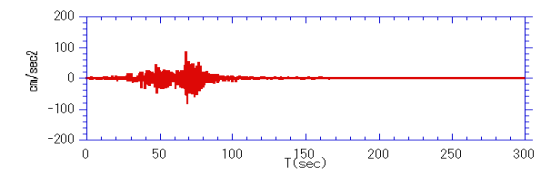
OBS.(N324.5E)



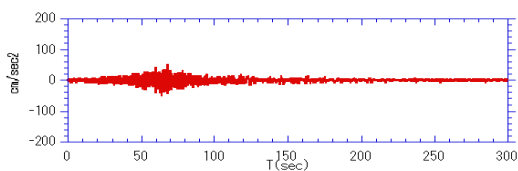
SYN.(N324.5E)



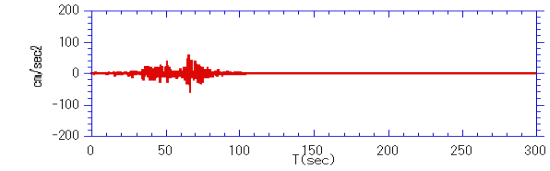
OBS.(N234.5E)



SYN.(N234.5E)



OBS.(UD)



SYN.(UD)

**Figure 5.2.** Comparison of observed and synthetic acceleration time histories for Shinjuku site

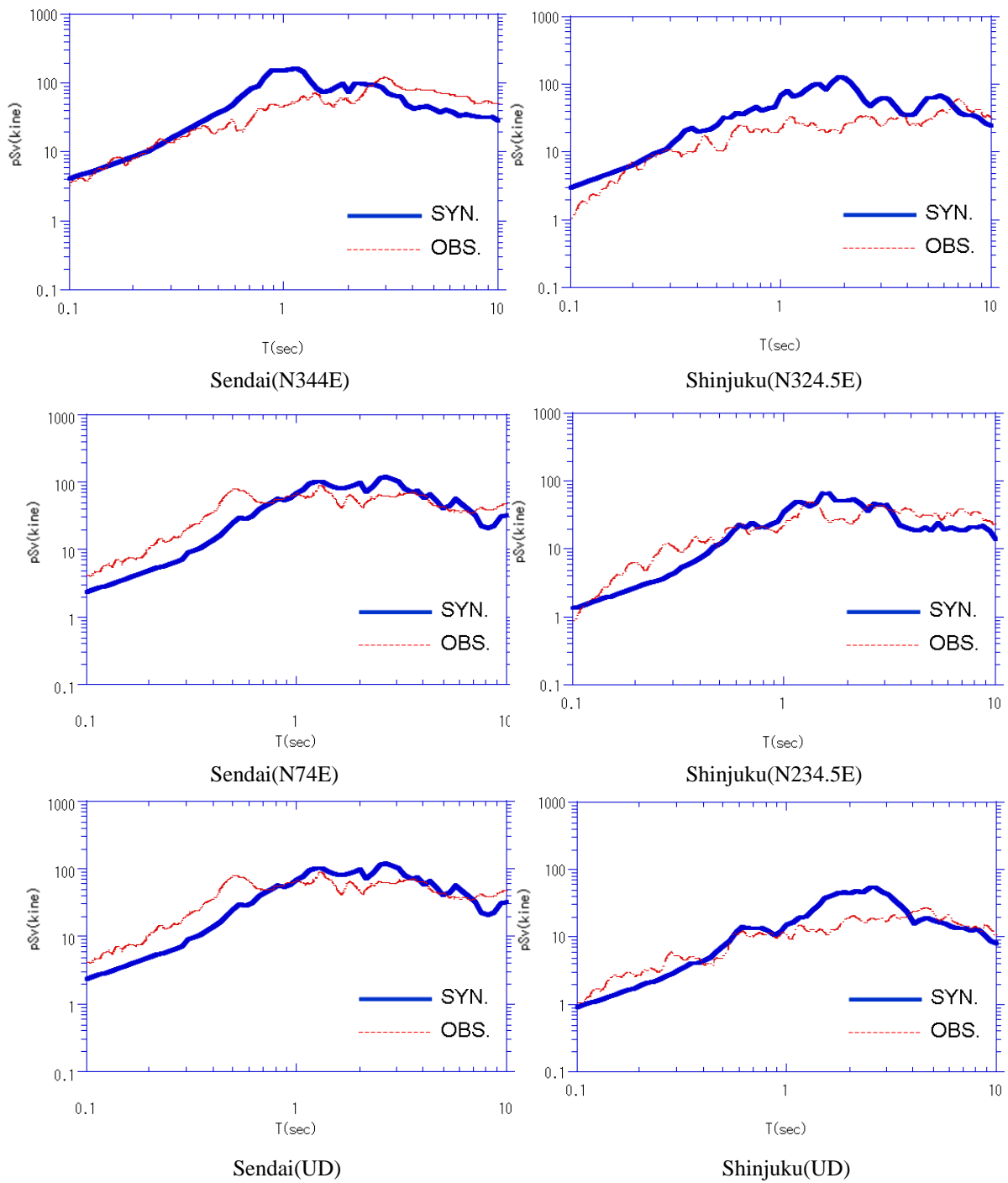


**Figure 5.3.** Comparison of observed and synthetic velocity response spectra for Sendai and Shinjuku site (damping ratio  $h = 5\%$ )

## 6. CONCLUSIONS

The ground motion model based on the wave propagation theory and source kinematics has been applied to simulate some ground motions of the 2011 off the Pacific coast of Tohoku Earthquake. The simultaneous simulation test has been applied to two sites by using the same source model. The ground motion model could describe the main portion of ground motions occurred by a large earthquake in ocean trench area.

Through the simultaneous simulation test, it is considered that the key parameters influencing characteristics of ground motion and structural response are the site geological structure from surface to deeper layer, focal distance, geometric relation between site and source, and asperity size and distribution on a fault plane.

## REFERENCES

- Kawano, M., Dohi, H. and Matsuda, S. (2000). Verification of predicted non-linear site response during the 1995 Hyogo-Ken Nanbu earthquake. *Soil Dynamics and Earthquake Engineering* **20**, 493-507.
- Dohi, H., Kawano, M., Asano, K. and Matsuda, S. (2004). Theoretical evaluation of attenuation relationship in distance for ground motion. *13th World Conference on Earthquake Engineering*, Paper No. 2553.
- Aki, K. and Richard, P.J. (1980). Quantitative seismology : theory and methods, **Vols 1 and 2**, Sausalito, California
- Seo, K., Yamanaka, H., Samano, T., and Midorikawa, S. (1988). Seismic prospecting of deep underground structure with explosions in the southwestern part of the Tokyo metropolitan area, Japan. *9th World Conference on Earthquake Engineering*, **Vol II**: 399-404.
- Koketsu, K. and Higashi, S. (1992). Three-dimensional topography of the sediment / basement interface in the Tokyo metropolitan area, Central Japan. *Bulletin of the Seismological Society of America*, **82**: **6**: 2328-2349.
- Kobayashi, K., Sato, Y., Uetake, T., Mashimo, M. and Kobayashi, H. (1997). Estimation of deep underground velocity structure in Sendai area by using earthquake records: Part 2 Inversion of spectral ratio of horizontal to vertical component. *Summarise of technical papers of annual meeting, Architectural Institute of Japan*, **B-2**, 185-186 (in Japanese)